PERGAMON

Journal of Structural Geology 22 (2000) 123–133

JOURNAL OF STRUCTURAL GEOLOGY

www.elsevier.nl/locate/jstrugeo

Structures on interfaces of mingled magmas, Stewart Island, New Zealand

John V. Smith

School of Resource Science and Management, Southern Cross University, P.O. Box 157, Lismore, 2480 NSW, Australia

Received 4 April 1998; accepted 4 April 1999

Abstract

Strain analysis of magmatic rocks has been attempted using the shapes of enclaves of contrasting magmas and analysis of mineral fabrics. In composite plutonic rocks of the Anglem Complex, Stewart Island, New Zealand, interfaces between different magma types are deformed into fold-like patterns which have the potential to provide new data on strain in magmatic processes. The fold-forms have shorter wavelength and higher amplitude on interfaces at a high angle to layering whereas fold-forms are either absent or of low amplitude on interfaces parallel to layering. The fold-forms may be amplified/de-amplified irregularities or buckle folds, and in either case they indicate shortening perpendicular to rock layering. Whole-rock fabrics of the plagioclase–hornblende–biotite rocks, analysed by shape preferred orientation and centre-to-centre methods, record less intense alignment and strain than predicted by free rotation of particles in viscous media. The inhibition of crystal rotation at high crystal concentrations and the growth of late poorly aligned crystals present difficulties for calibrating whole-rock fabrics with the strain incurred by magmatic flow.

1. Introduction

Strain analysis is founded on the principle that the present configuration of features in rock can be compared to some previous configuration(s) of the same features to record the change(s) of shape which have occurred in that rock. In metamorphosed sedimentary rocks features such as beds and fossils provide excellent markers for strain analysis. In magmatic rocks there is no definable 'original' configuration nor are intermediate configurations easily recognised to provide a framework for strain analysis. Two approaches to strain analysis in magmatic rocks have been (1) measurement of the shapes of enclaves of contrasting magma within a pluton and (2) petrographic analysis of rock fabrics.

There has been strong support for the interpretation that enclaves of contrasting magma type and their host rocks commonly form by mingling together in the molten state (Vernon et al., 1988), particularly as a result of syn-plutonic intrusion (Wiebe, 1993; Wiebe and Collins, 1998). Enclaves commonly have irregular lobate forms resulting from viscous break-up of magma (Vernon et al., 1988). Analysis of the ellipticity and orientation of enclaves has been used to infer a pre-deformation distribution of shapes and orientations of an enclave population (Bateman, 1983; Fernandez and Barbarin, 1991). The relationship between enclave shape and petrographic fabric in some enclaves is complex; for example, Vernon (1991) described crenulate enclave margins within which the fabric was parallel to the margin.

The modelling of fabrics of aligned minerals in rocks as the rotation of particles in a viscous media has a long history (Jeffery, 1922; Gay, 1968). With specific reference to plutonic rocks, experiments have been used to refine these models by recognising other influences, such as particle interactions (Ildefonse et al., 1992; Fernandez and Fernandez-Catuxo, 1997). Fernandez and Laporte (1991) reported studies that analysed subfabrics comprising populations of particular minerals within the rock fabric. However, the nature and timing of magmatic fabrics in plutons are

E-mail address: jsmith1@scu.edu.au (J.V. Smith)

0191-8141/00/$ - see front matter
PII: S0191-8141(99)00139-X

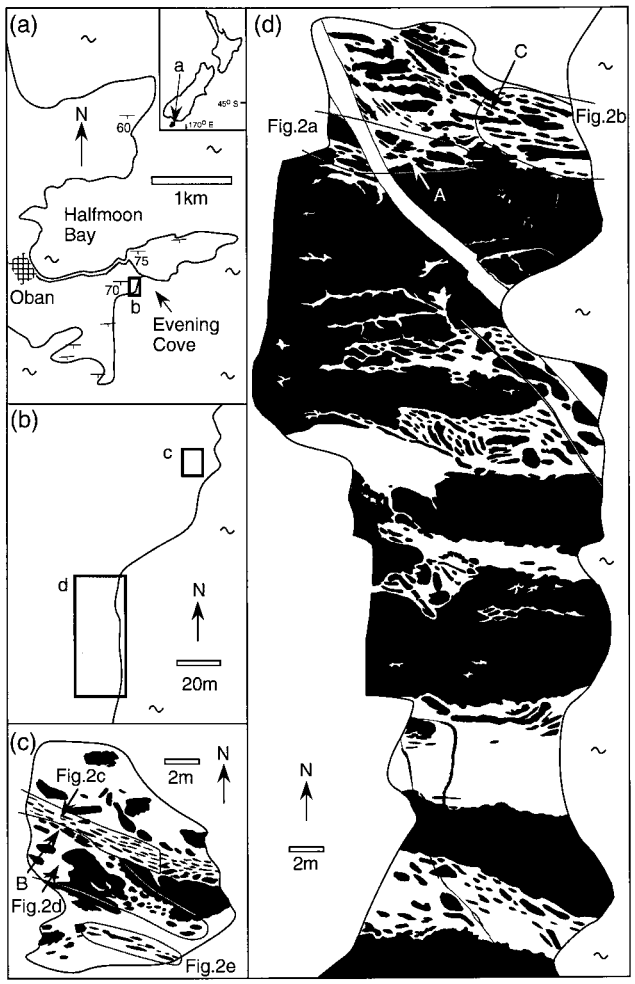

Fig. 1. Location map for Stewart Island and detailed geological maps of composite plutonic rocks composed of gabbroic to dioritic rocks (black) and tonalitic rocks (white) exposed at Evening Cove, Stewart Island (foliation trends in (a) are taken from Watters, 1978).

not sufficiently well understood to allow unequivocal interpretation without reference to other internal features. Fowler and Paterson (1997) compared fabric intensity and orientation with respect to stoped xenoliths in granites and concluded that the foliation reflected only the latest stages of emplacement.

The presence of interfaces between magmas of different composition provides the possibility of measuring components of magma movement in more detail than is possible for a homogeneous magma. The analysis of features of deformed interfaces can potentially provide a great deal of information about the mechanical behaviour of geological material (Treagus, 1981; Cobbold, 1983). Biot (1961) and Ramberg (1963) recognised that the viscosity contrast between materials is an important influence on the development of folds in layered materials. Ramsay and Huber (1987, p. 418) used the term 'cuspate–lobate folds' to describe folds that occur in layers of relatively low viscosity contrast. The wavelengths and amplification rate of such folds are so low that the folds that occur on interfaces need not be in phase on upper and lower surfaces of a layer. Thus, these folds develop independently on each interface and do not require the presence of multilayers in order to form.

Table 1
Whole-rock geochemistry of (1) mafic enclave, (2) felsic host rock of specimen A, (3) intermediate enclave, (4) felsic host rock of specimen B. Analysis by ICP-MS, Amdel Australia

	1	2	3	4
SiO_2	50.0	54.3	51.4	58.8
Al_2O_3	18.4	21.3	19.1	19.8
CaO	8.12	6.21	8.39	6.97
Fe_2O_3	10.7	6.60	9.02	5.06
MnO	0.16	0.06	0.15	0.07
MgO	3.98	1.95	2.92	1.55
TiO_2	1.47	0.775	1.27	0.620
K_2O	1.32	1.54	0.68	0.81
Na_2O	3.92	5.10	4.34	4.62
P_2O_5	0.65	0.27	0.46	0.22
LOI	0.98	0.73	0.95	1.34
Total	99.7%	98.8%	98.7%	99.9%

Considerations of the cooling histories of different magmas have enabled the development of detailed models of the mechanical interactions of magma types as their absolute and relative rheologies change (Fernandez and Gasquet, 1994). Williams and Tobisch (1994) modelled the effects of contrasting magma compositions, temperature and magma flow velocities using drop deformation theory. They concluded that enclaves record magmatic strain of the host over only a limited temperature–time range in the host's cooling history. They proposed that the rates of magma flow would be low, but may be higher if shear thinning rheology applied. Smith (1997) proposed that shear thickening is expected in a crystal mush which supports a low flow rate in plutonic flows.

In this paper, fold-like structures on the interfaces between contrasting magma types of the Anglem Complex of Stewart Island, New Zealand (Fig. 1) are investigated and their potential as strain markers in plutonic rocks is considered. Preliminary comparisons between these structures and the results of analyses of enclaves and whole-rock fabric are discussed.

2. Geological setting

The northern part of Stewart Island, New Zealand, is dominated by plutons of the Anglem Complex, which are composed of tonalites, diorites and hornblende gabbros (Watters, 1962, 1978). These Cretaceous intrusions are complexly interrelated and have been interpreted as the result of magma mingling

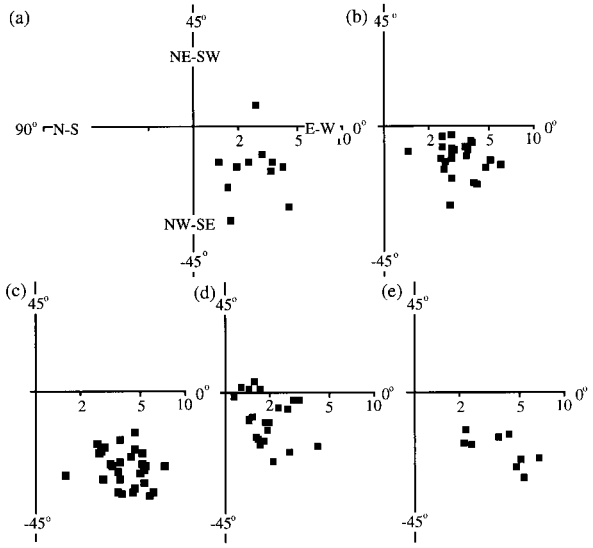

Fig. 2. Double angle–log polar plots of the R_f/ϕ_f values determined by analysis of discrete enclaves in the domains encircled in Fig. 1(c) and (d).

(Cook, 1988). A section through one part of the composite magma is well exposed at Evening Cove, 2 km southeast of Oban, the main settlement on Stewart Island (Fig. 1).

Geochemical analyses of two pairs of adjacent enclave and felsic host rock (Analyses 1 and 2 from Specimen A and Analyses 3 and 4 from Specimen B) are presented in Table 1. Specimen A enclave is an olivine normative, evolved tholeiitic basalt enclave. This composition may approximate the mafic liquid composition although the high K_2O (and H_2O) probably reflects exchange with felsic magma. Specimen A felsic host rock has very high Al_2O_3 suggesting it is a feldspar cumulate. If compaction was involved (e.g. McKenzie, 1987), some of this character could be explained by filter-pressing of interstitial liquid and movement of that liquid upward either back into the magma chamber or into overlying mafic bodies. Specimen B is intermediate and may be a hybrid version of the mafic enclave (Analysis 1) because of similar but lower amounts of MgO, TiO_2 and P_2O_5 not due to simple bulk contamination because this enclave is lower in K_2O than Analysis 1. Specimen B felsic host rock has similarities to Analysis 2 but has higher normative quartz and somewhat less total normative feldspar. The Al_2O_3 is still quite high and the normative mineralogy suggests that this rock is also a feldspar cumulate, possibly with more trapped liquid.

The mafic layers and enclaves within the Anglem Complex have been interpreted as replenishments of magma emplaced on a crystal-rich chamber floor (Wiebe and Collins, 1998). Some of the mafic layers show evidence for upward (southward) increase in hybridisation with the tonalite (increasing proportions of feldspar xenocrysts) and a rubbly to pillowed upper surface (Fig. 1).

3. Enclave shapes

As illustrated in Fig. 1, the distribution of the contrasting magma types is complex and discrete enclaves are not dominant. The layering defined by the contrasting magma types dips 70° to the south. The exposure surfaces slope gently northward and photographic images were taken down-dip so no correction is required for the orientation of the structures relative to the exposure. The shape analysis described below is for the two dimensions of the exposure only.

Enclave shapes (aspect ratios) and orientation (long axis) were measured for five domains (Fig. 1) of discrete enclaves. Double angle polar plots (Fig. 2) of the enclave shapes and orientations contrast the relatively low to moderate aspect ratios (R_f 2 to 5) of enclaves trending near east–west (Fig. 2a, b, d) with the relatively high aspect ratios (R_f 5 to 9) of enclaves trending east-southeast. The ranges of orientations at low aspect ratio indicate that the enclaves did not originate as spherical (circular) objects.

4. Interfacial fold-forms

The gross pattern of magma interfaces (Fig. 1) reflects the complex mingling of magma types. On a detailed scale, the interfaces range from smooth to fold-like. The highest amplitude fold-forms occur on interfaces oriented at a high angle to the dominant east–west layering (Fig. 3a) of the magma types and low amplitude fold-forms or smooth interfaces occur on interfaces parallel to the layering. On oblique interfaces the wave-forms are asymmetric (Fig. 3b).

The high amplitude wave-forms are interpreted as the result of interface-parallel shortening on the parts of interfaces at a low angle to shortening direction. This may have occurred by either buckling of smooth interfaces (Fig. 4a, b and c) or by amplification of irregularities (Fig. 4e and f). These processes, separately or together, account for the folded appearance of magma interfaces and the inferred concertina or paper-lantern-like three-dimensional morphology (Fig. 4g).

4.1. Buckle folding

Analyses of geological folds do not generally address the effects on an interface in isolation, but are based on two or more parallel interfaces that define layered systems. Ramsay and Huber (1987, p. 418) commented that where viscosity contrast is small, the wavelength

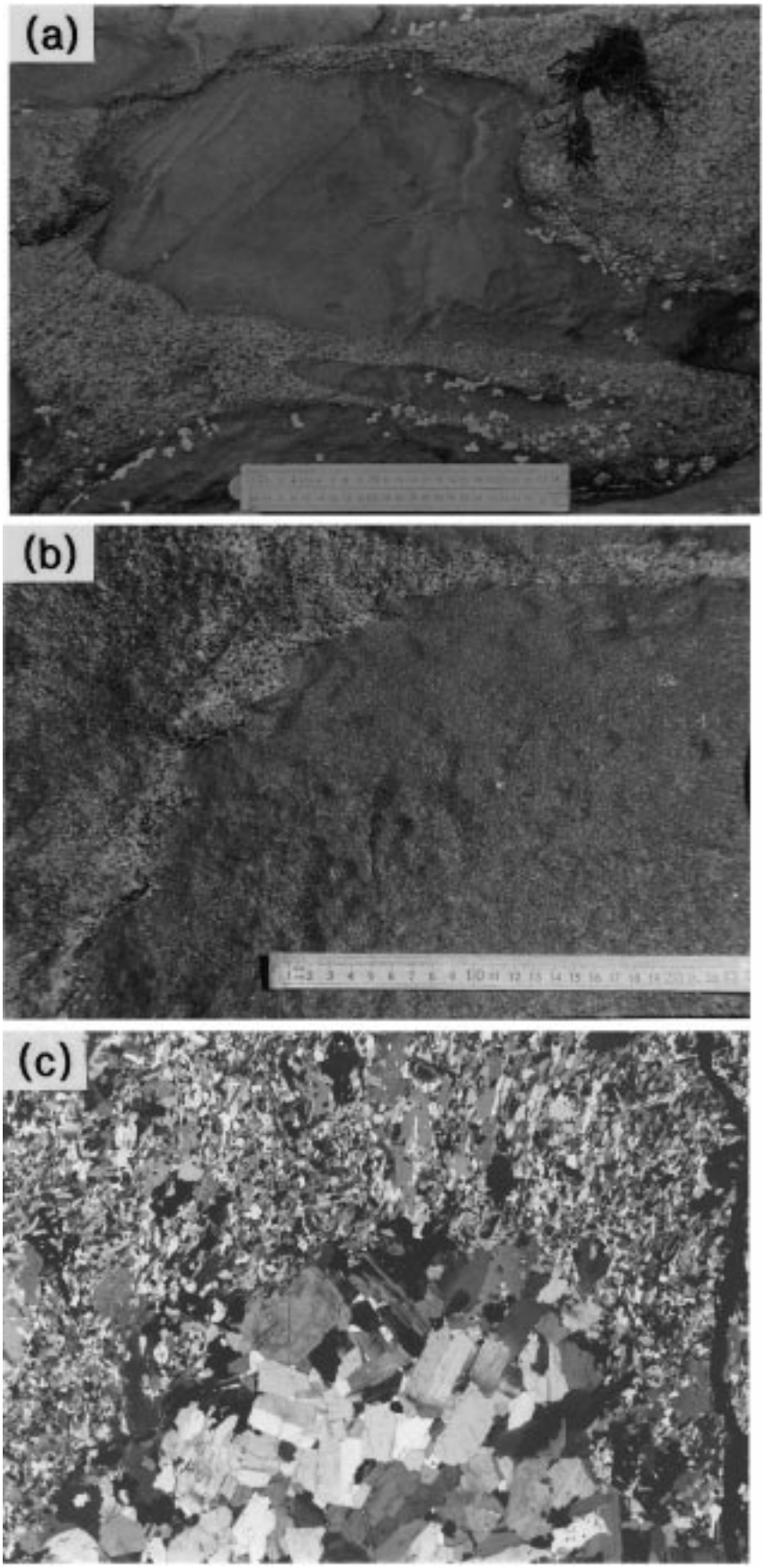

Fig. 3. (a) Field photograph of an enclave with low-amplitude fold-forms on interfaces parallel to magmatic layering (parallel to bar scale) and high-amplitude fold-forms on interfaces at a high angle to magmatic layering (left of photograph). (b) Asymmetric folds on a magma interface (bottom left to top right) oriented obliquely to magma layering (parallel to scale) separating mafic (bottom right) and felsic (top left) rocks. (c) Photomicrograph (crossed polars) of a folded magma interface in Specimen A separating fine-grained mafic (top) and coarse-grained felsic (bottom) minerals. Field of view 10 mm across.

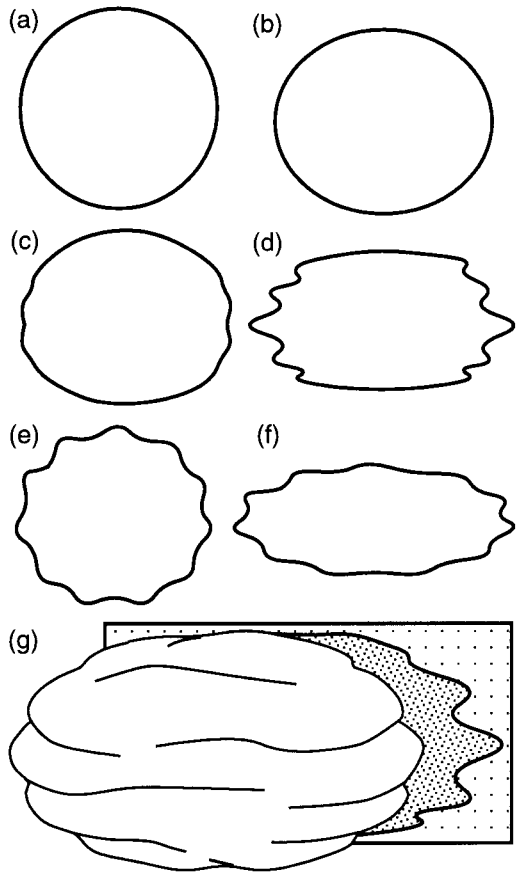

Fig. 4. (a) An enclave with a smooth interface may (b) retain the smooth interface during deformation or (c) develop buckle folds on lateral interfaces which (d) amplify with further flattening. (e) Irregularities on enclave interfaces are (f) amplified on lateral surfaces and de-amplified on longitudinal surfaces. (g) The resulting three-dimensional morphology of the flattened enclaves resembles a concertina or paper lantern.

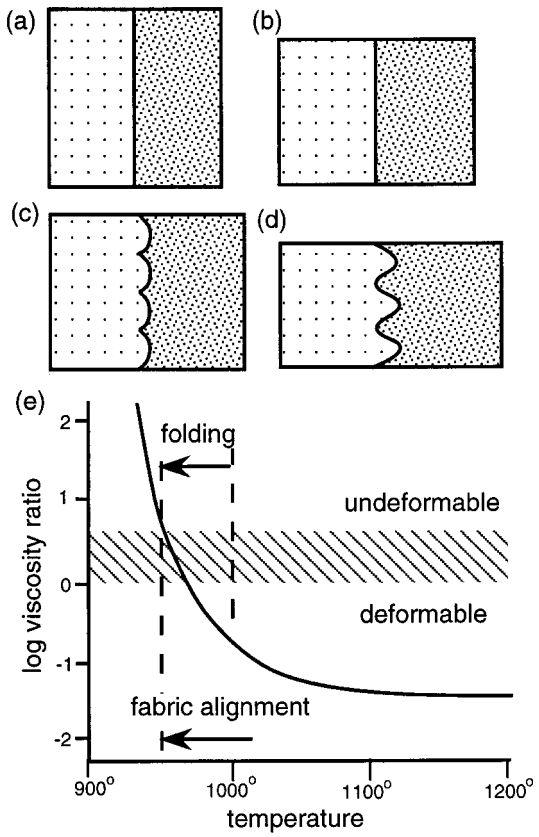

Fig. 5. (a) Illustration of an interface between a silicic (light stippling) and relatively mafic (heavy stippling) magma. Interface-parallel shortening with (b) no viscosity contrast would be homogeneous whereas, (c) a high viscosity contrast (low viscosity mafic component) would produce cuspate–lobate interface folds. (d) Symmetrical fold-forms imply overall equivalence of viscosities, implying formation over an interval spanning the viscosity equality point as shown in (e). (e) Representative relationship between the (log) ratio of viscosities of composite magmas showing inferred temperature ranges of interface folding and fabric alignment. The onset of undeformability of the more mafic component (56.8% SiO_2 in this example) is taken from Williams and Tobisch (1994).

of folding of interfaces is so short that it is commonly much less than the thickness of layers, and the folds on each surface of a layer are 'decoupled' and may be out of phase (disharmonic). Consequently, the analysis of these type of folds is not only applicable to layers, but may be applicable to folding of interfaces of other configurations such as the margins of enclaves.

Analysis of the interface fold-forms requires consideration of the viscosity contrast indicated by the shape of the folds. If there were no viscosity contrast buckle folds would not develop (Fig. 5a and b). For a low viscosity contrast (in the sense of Ramsay and Huber, 1987, p. 418) small wavelength cuspate–lobate folds would develop (Fig. 5c). The degree of difference in fold shape between the rounded lobes and the angular cusps is an indication of the magnitude of the viscosity ratio. The symmetrical interface folds observed at Evening Cove are therefore problematic, as the symmetry implies no viscosity contrast, but that should result in no folding. This problem is resolved by considering the nature of the viscosity contrast as temperature decreases. At high temperature the more mafic magma has a lower viscosity, but as it moves toward crystallisation the more siliceous magma becomes relatively less viscous. If the folding occurs over an interval spanning the viscosity cross-over, the cuspate–lobate tendencies would reverse and the final result could be symmetrical interface folds (Fig. 5d and e).

Theoretical modelling (Williams and Tobisch, 1994) suggests that soon after the viscosity cross-over, when the viscosity contrast is between 1 and 4, the mafic magma becomes undeformable (Fig. 5e, shading). Therefore, if an approximately equivalent amount of shortening occurs before and after the viscosity cross-over (as indicated by the symmetry of interface folds), an approximate temperature range of folding can be inferred (Fig. 5e).

Low viscosity contrast folding is characterised by

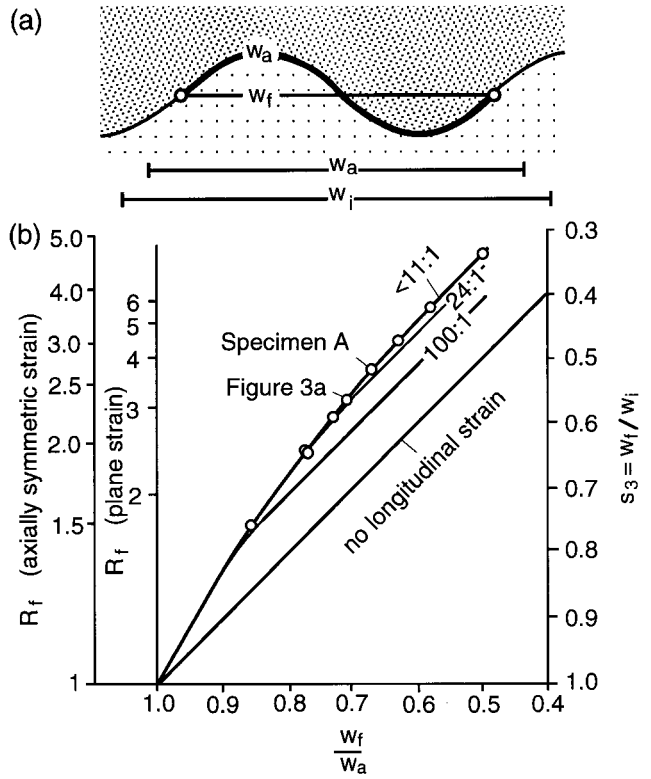

Fig. 6. (a) Illustration of the relationship between the fold wavelength (w_f) and the arc length (w_a). The initial wavelength (w_i) is greater than w_a if homogeneous layer-parallel shortening has occurred. (b) Graph relating arc-length measurements to actual contractions in viscous materials based on experiments of Hudleston (1973). Within the range of strain considered, low viscosity contrast systems share a common curve. Open circles are data from fold-forms on lateral margins of enclaves.

having a high component of homogeneous interface-parallel shortening, in addition to the effects of fold limb rotation (Hudleston, 1973). Therefore, analysis of the folds by the arc-length method, in which the final wavelength (Fig. 6a, w_f) is divided by the length of the fold arc (Fig. 6a, w_a), underestimates the actual strain, which is related to the true initial wavelength (Fig. 6a, w_i). Hudleston (1973) performed experiments to determine these relationships. He found that interface-parallel shortening commonly formed by a sequence of early homogeneous longitudinal strain followed by fold development. The magnitude of the longitudinal strain was found to depend on the viscosity contrast, and a common relationship is shared by systems with a low viscosity contrast (less than 11:1), of interest in this study (Fig. 6b). The arc-length method can overestimate shortening if the interface was not originally straight. If the pre-folding surface were the perimeter of a quadrant of a circle, simple geometric analysis indicates that the assumption of a straight line would result in a 10% overestimate of strain. However, this effect would also be evidenced by asymmetric folds, and since the folds analysed were of symmetric form I propose that no substantial overestimate of strain has occurred by this effect.

The rotation of the interface by folding may be a plane strain effect, whereas the bulk (average) strain is probably triaxial and may be approximately axially symmetric. Therefore, to convert the total shortening to a strain ellipse, the two components would be determined separately and recombined to give a total strain ellipse of folding. For simplicity it will be assumed that constant volume is maintained, although volume may change by processes such as melt migration (McKenzie, 1987).

Measurements were made from eight field examples using photographs and one thin section (Specimen A) (Table 2). The arc-length shortening values were plotted on the low viscosity contrast folding curve (Fig. 6b, open circles) to determine values of total shortening stretch which ranged from 0.32 to 0.77 with an average value of 0.68. The variation may be due to uncontrolled factors, including measurement errors, but it is also possible that the variation is systematic due to such factors as the compositional contrast

Table 2
Data from field measurement (and thin section in the case of specimen A, labelled) of the wavelength, amplitude, arc-length stretch and longitudinal shortening corrected for homogeneous shortening (Hudleston correction). Standard deviations of means given in brackets

Identification	Wavelength mm (av.)	Amplitude mm (av.)	Arc-length stretch	Longit. shortening (Hudleston correction)
Specimen A	21	11	0.67	0.51
	27	24	0.50	0.32
	26	21	0.59	0.40
	23	11	0.63	0.48
	25	9	0.73	0.59
	30	17	0.77	0.62
	18	7	0.86	0.77
	35	25	0.77	0.62
Fig. 3(c)	42	28	0.71	0.55
			0.68 (0.13)	0.54 (0.12)

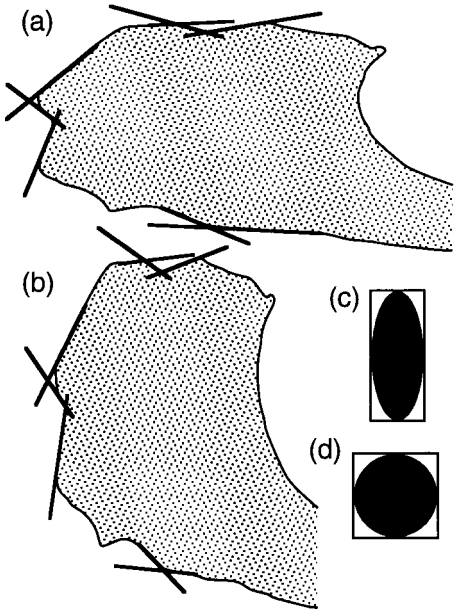

Fig. 7. (a) The final shape of the enclave in Fig. 3(a) with interlimb angles of interface fold-forms marked on lateral and longitudinal faces. (b) Retrodeformation of the enclave to produce equivalent interlimb angles on all faces. The strain is illustrated by equivalent (c) deformed and (d) undeformed ellipses.

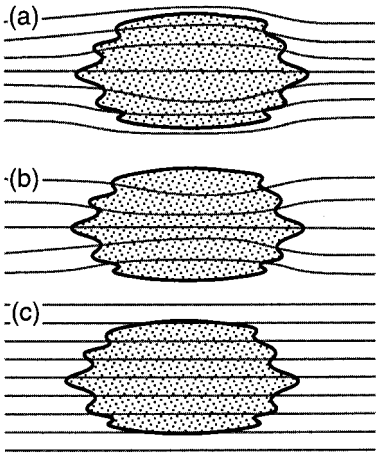

Fig. 8. Strain relations between enclaves and hosts showing pattern of foliation with (a) less strain in enclave, (b) greater strain in enclave and (c) equal strain.

between magma types or systematic strain gradients in the outcrop.

4.2. Amplification/de-amplification of irregularities

It is possible that the fold-forms developed, not by buckle folding but by the amplification and de-amplification of irregularities on magma interfaces. Figures 3(a) and 7(a) show an enclave with interface irregularities around its margin. The interlimb angle of the folds on interfaces parallel to the layering is greater than that of the interface perpendicular to the layering. The maximum and minimum interlimb angles can be used to estimate the strain (Fig. 7b–d, Ramsay and Huber, 1983, p. 138). For this example, $R = 2.4$ and, for plane strain, the least principal stretch $(s_3) = 0.65$. The arc-length value for the fold on the left-hand side of the figure is 0.71 with a Hudleston correction to 0.55. Analysis of numerous enclaves would be required to determine the mechanism by which the fold-forms developed and to overcome random variations in shapes.

5. Whole rock fabric

The use of rock fabric as a record of flow is based primarily on experimental and theoretical work, which either considers the orientation of particles (Jeffery, 1922; Gay, 1968; Shelley, 1993) or the distribution of particles (Fry, 1979; Ribeiro et al., 1983, Erslev, 1988). The use of both these methods has been invigorated by the application of digital image analysis techniques (Alliers et al., 1995; Bons and Jessel, 1996). Fernandez and Laporte (1991) analysed the orientation of specific mineral constituents, whereas in this work the whole rock texture is analysed.

Theoretical and experimental work has shown that ideally the ellipse that characterises the degree of alignment of rigid particles is related to the strain ellipse for coaxial flow (Gay, 1968). For low concentrations of highly elongate particles, the alignment ellipse can be approximately equal to the strain ellipse. Decreasing aspect ratio and increasing particle concentration both tend to cause the alignment ellipse to be less than the strain ellipse. A two-dimensional analysis of the relationship between particle alignment and strain is given by Ildefonse et al. (1992) and three-dimensional relationships with simple shear strain have been investigated by Fernandez and Fernandez-Catuxo (1997).

The pattern of fabric orientation with respect to contrasting magma types allows some interpretations of the distribution of strain to be made. For example, where a magma enclave is less strained than the host magma, the strain-related fabric would be deflected around the enclave (Fig. 8a; Sen, 1956), where a magma enclave is more highly strained than the host magma, strain-related fabric would be deflected into the enclave (Fig. 8b) and where the strain is equivalent in each magma type the fabric would pass through magma interfaces undeflected (Fig. 8c). At Evening Cove, the aligned fabric observed in the field was parallel to the dominant layering defined by elongated magma bodies and was undeflected across magma interfaces, suggesting equivalent strain in each magma

Table 3
Fabric analysis of specimens containing interfaces. The ellipticity of the alignment of crystals (R_f) and its orientation (ϕ_f), the average aspect ratio, interpreted longitudinal shortening (s_3), ellipticity of centre-to-centre analysis (R_l) and its orientation (ϕ_l). Twice standard error is given in brackets. Significance of orientation data is too low to allow detailed comparisons of fabric orientations

	n (grains)	Mean R_f	Mean ϕ_f	Aspect ratio	s_3	n (lines)	R_l	ϕ_l
Specimen A (enclave)	138	1.53	−10.7	2.33	0.71	312	1.52	−13.6
		(0.15)	(5.6)	(1.21)			(0.20)	(8.2)
Specimen A (host)	223	1.18	−16.5	1.89	0.87	505	1.14	−9.7
		(0.12)	(13.1)	(0.70)			(0.14)	(26.9)
Specimen B (enclave)	99	1.29	−13.1	2.07	0.81	224	1.29	−17.2
		(0.15)	(9.7)	(0.80)			(0.20)	(16.4)
Specimen B (host)	133	1.14	−22.93	1.86	0.91	315	1.08	−24.0
		(0.10)	(17.4)	(0.61)			(0.12)	(38.7)

type. This observation allows direct comparison of the intensity of fabrics in contrasting magma types.

Paterson et al. (1989) proposed criteria that can be used to determine the state of the magma at the time the fabric was formed. Principally, the presence of crystal alignment without evidence of plastic deformation or recrystallisation is typical of fabrics which formed in the magmatic state. The only evidence of solid-state deformation observed in specimens was weak distortion of some of the longest feldspar grains, evidenced by slightly undulose extinction patterns and I conclude that the fabric of the rocks in this study was produced by flow in the magmatic state.

The fabric in two specimens, which both include magma interfaces, was studied in thin sections. Specimen A (Fig. 1d) contains a folded hornblende gabbro–tonalite interface oriented perpendicular to the main trend of layering. Specimen B (Fig. 1c) includes two interfaces between diorite bodies separated by tonalite. The interfaces in specimen B are oriented par-

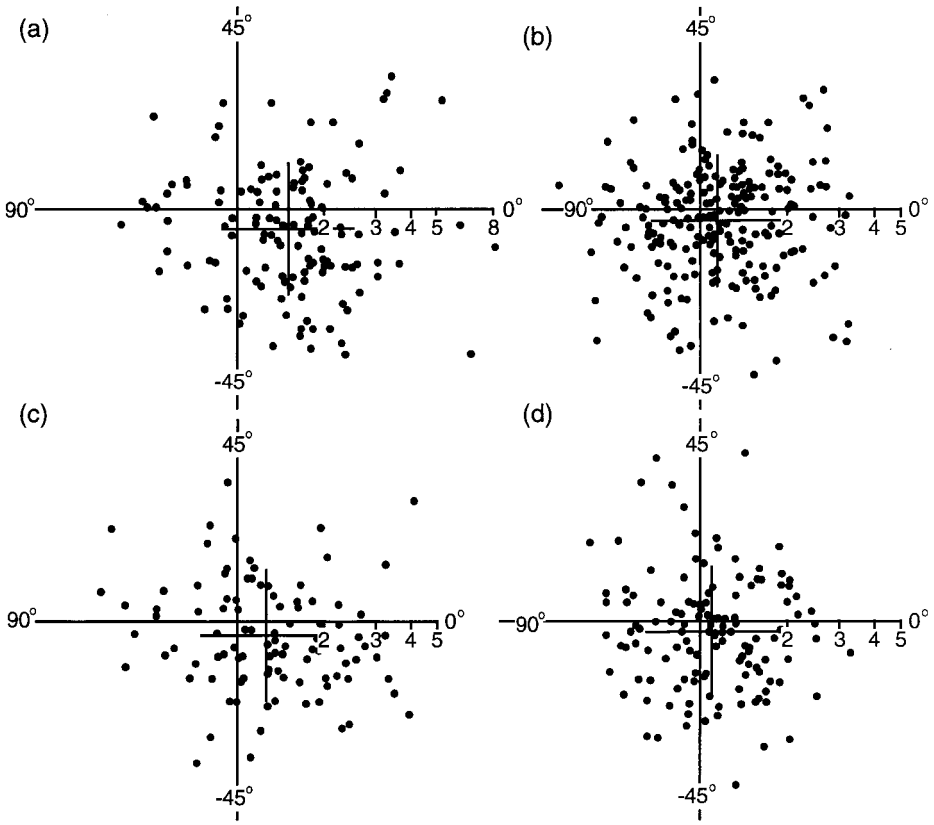

Fig. 9. Double angle–log polar (Elliott) plots of the R_f/ϕ_f values determined by fabric analysis of the samples (Table 3). (a) Specimen A enclave, (b) Specimen A host, (c) Specimen B enclave and (d) Specimen B host.

allel to the main trend of layering. The three main rock types and grain sizes are represented in the specimens and the two main orientations of interfaces with respect to layering are also represented. Thin sections were cut perpendicular to layering approximately parallel to the sub-horizontal exposure surface. Thin sections were also cut perpendicular to layering in the down-dip direction. No significant difference in the shape and degree of alignment of crystals was observed in the mutually perpendicular thin sections indicating that the fabric is approximately axially symmetric. The sub-horizontal sections were analysed in detail for comparison with the observed magma interface structures. Line drawings were prepared from base photomicrographs with reference to the microscope to differentiate crystal boundaries from twin boundaries. Digital images 640 by 480 pixels were taken from the line drawings. Incomplete grains along image boundaries were discarded and a cut-off size of 400 pixels was used to facilitate the image processing.

The two-dimensional fabrics were analysed using the image processing system developed by Dr D.W. Durney. The system analyses both the grain-shape orientation fabric (R_f/ϕ_f) and nearest neighbour centre-to-centre length anisotropy (R_l/ϕ_l). The former measures the mean shape anisotropy of the grains whereas the latter measures the relative distribution of grain centres. In both methods the intensity of the measured fabric is defined by an ellipticity (R) and the orientation is defined by the position of the long axis of the ellipse (ϕ).

The analysis shows mean R_f values ranging from 1.14 to 1.53 and mean ϕ_f values ranging from -10.7 to -22.9°, with respect to an arbitrary datum, namely the long edge of the thin section. R_l values range from 1.08 to 1.52 and ϕ_l values range from -9.7 to -24.0° (Table 3). The R_f/ϕ_f data are illustrated in the form of double angle–log polar plots (Fig. 9). These plots illustrate the way the individual grains represent a range of shapes and orientations which can be characterised by a mean value (Elliott, 1970). The mean value is obtained by iterative unstraining of the deformed distribution to one with a zero mean vector (isotropic).

The differences in fabric orientation within specimens are within the values of twice the standard error, and a study with more orientation data would be required to determine whether subtle systematic changes in orientation actually exist. Deflections of the fabric would indicate disparities in strain magnitude between magma types, as discussed above.

The poor definition of alignment in the rock fabric relative to enclave shapes and interfacial fold-forms may be a consequence of the following factors. (1) The progressive nucleation and growth of crystals during cooling could cause the recorded strain to lag behind that predicted for a static population of particles. (2)

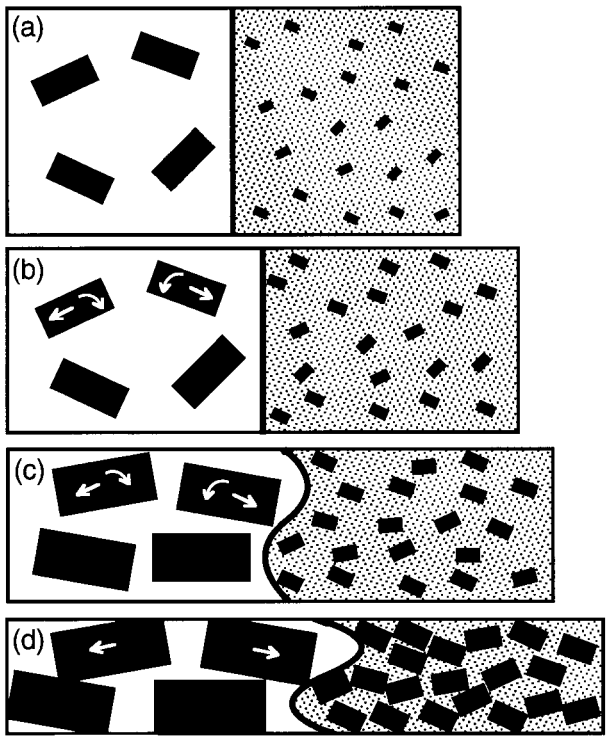

Fig. 10. Stages of structural development. (a) The initial configuration of crystals (black rectangles) is unknown and transient structures and fabrics may have existed. A randomly oriented anticlustered distribution is taken as a notional initial state. (b) Bulk flattening rotates and translates crystals creating an aligned fabric while magma interfaces (centre line) at high angles to the layering of the mingled magmas undergo homogeneous interface-parallel shortening. (c) Interface buckling initiates and develops as fabric continues to develop. (d) Interface buckling continues but crystal concentration becomes so great that crystal rotation is inhibited and fabric is distorted primarily by translation (arrows) of crystals.

The formation of crystals without a shape preferred orientation, such as anhedral space-fillings, could decrease the recorded fabric alignment. (3) Crystal rotation could be greatly inhibited at high crystal concentrations. Anhedral space-fillings have a strong influence on the fabric of quartz-bearing rocks (Paterson et al., 1989), but the rocks described here are very poor in quartz. However, the shape-orientation of some subhedral feldspar crystals, for example, may be controlled by space-filling rather than free rotation, particularly at high crystal concentrations. Such a process might also be controlled by the pulling apart of the crystal mush to produce overgrowths and other space-filling fabrics. Late overgrowths of Na–plagioclase were observed by Vernon (1991) and with further petrological investigations these features may be amenable to analysis in the way overgrowths are commonly used in strain analysis of deformed clastic sedimentary rocks. The inhibition of crystal rotation with increasing concentration was stu-

died with analogue models by Ildefonse et al. (1992). They found approximately 10% underestimate of strain due to inhibition of particle rotation when the particle concentration was sufficiently high to cause approximately 40% of particles to undergo a collision with neighbours. The degree of inhibition of particle rotation at higher concentrations may be even greater.

While particle concentrations are relatively low (Fig. 10a), flow is accompanied by rotation and translation of particles (Fig. 10b). During this time sufficient longitudinal strain may accumulate to allow interface folding to initiate (Fig. 10c). As the particle concentration increases, particle rotation is impeded and flow occurs dominantly by translation of particles (Fig. 10d). Any fabric deformation occurring by crystal translation is not recorded in the degree of alignment of the crystals. This type of deformation is commonly analysed by centre-to-centre methods. However, the analysis included in this study found that centre-to-centre values were similar to the results of the crystal alignment method. Theoretical and analogue modelling of the kinematics of densely concentrated suspensions may be required to determine whether the strain not recorded by the fabric analysis could have occurred in this way. If so, it may also be possible to reassess the application of centre-to-centre methods to attempt to incorporate this effect in fabric analyses. Grain size and shape possibly could be used to select grains that might best record strain in plutonic rocks. However, neither of these features is necessarily directly related to order of crystallisation (Flood and Vernon, 1988).

6. Discussion and conclusions

The data presented here indicate that an important part of the mingling of the composite magmas was approximately coaxial flattening aligned with the magmatic layering in the final stage of solidification. Preliminary analyses suggest that approximately 50% shortening occurred in this way as recorded by fold-forms on magma interfaces. The shapes of enclaves and rock fabric may be strongly influenced by earlier, more chaotic, kinematics of magma mingling and comparison of all these features may lead to an improved understanding of magma chamber dynamics.

Although magmatic rocks may seem poor candidates for strain analysis, the fold-forms on the interfaces between contrasting magma types, introduced in this paper, provide a possible reference by which to evaluate studies of enclave shapes and rock fabrics. A more comprehensive study of the interfacial fold-forms is required to determine whether they are produced by buckle folding or amplification/de-amplification of irregularities.

Acknowledgements

I thank David Durney for generous assistance with use of his original image processing and strain analysis software, suggesting amplification/de-amplification effects and indicating limitations in fabric analysis. Robert Wiebe provided helpful discussions on the geology of Stewart Island and calculation of normative mineralogy and Richard Flood assisted in interpretation of plutonic textures. These colleagues and Ron Vernon provided helpful comments on an early version of the manuscript although the views and conclusions expressed are entirely the responsibility of the author.

References

Alliers, L., Champenois, M., Macaudiere, J., Bertrand, J.M., 1995. Use of image analysis in the measurement of finite strain by the normalised Fry method: geological implications for the 'Zone Houilliere' (Brianconnaise zone, French Alps). Mineralogical Magazine 59, 179–187.

Bateman, P.C., 1983. A summary of critical relations in the central part of the Sierra Nevada batholith, California, U.S.A. Geological Society of America Memoir 159, 241–254.

Biot, M.A., 1961. Theory of folding of stratified viscoelastic media and its implications for tectonics and orogenesis. Geological Society of America Bulletin 72, 1595–1620.

Bons, P., Jessell, M.W., 1996. Image analysis of microstructures in natural and experimental samples. In: De Paor, D.G. (Ed.), Structural Geology and Personal Computers. Pergamon Press, Oxford, pp. 135–166.

Cobbold, P.R., 1983. Kinematic and mechanical discontinuity at a coherent interface. Journal of Structural Geology 5, 341–349.

Cook, N.D.J., 1988. Diorites and associated rocks in the Anglem Complex at The Neck, northeastern Stewart Island, New Zealand: an example of magma mingling. Lithos 21, 247–262.

Elliott, D., 1970. Determination of finite strain and initial shape from deformed elliptical objects. Geological Society of America Bulletin 81, 2221–2236.

Erslev, E.A., 1988. Normalized centre-to-centre strain analysis of packed aggregates. Journal of Structural Geology 10, 201–209.

Fernandez, A.N., Barbarin, B., 1991. Relative rheology of coeval mafic and felsic magmas: nature of resulting interaction processes and shape and mineral fabrics of mafic microgranular enclaves. In: Didier, J., Barbarin, B. (Eds.), Enclaves and Granite Petrology, Developments in Petrology 13. Elsevier, Amsterdam, pp. 263–275.

Fernandez, A., Gasquet, D.R., 1994. Relative rheological evolution of chemically contrasted coeval magmas: example of the Tichka plutonic complex (Morocco). Contributions to Mineralogy and Petrology 116, 316–326.

Fernandez, A., Fernandez-Catuxo, J., 1997. 3D biotite shape fabric experiments under simple shear strain. In: Bouchez, J.L., Hutton, D.H.W., Stephens, W.E. (Eds.), Granite: From Segregation of Melt to Emplacement Fabrics. Kluwer, Dordrecht, pp. 145–157.

Fernandez, A., Laporte, D., 1991. Significance of low symmetry fabrics in magmatic rocks. Journal of Structural Geology 13, 337–347.

Flood, R.H., Vernon, R.H., 1988. Microstructural evidence of orders of crystallization in granitoid rocks. Lithos 21, 237–245.

Fowler, T.K., Paterson, S.R., 1997. Timing and nature of magmatic

fabrics from structural relations around stoped blocks. Journal of Structural Geology 19, 209–224.
Fry, N., 1979. Random point distributions and strain measurements in rocks. Tectonophysics 60, 89–105.
Gay, N.C., 1968. The motion of rigid particles embedded in a viscous fluid during pure shear deformation of the fluid. Tectonophysics 5, 81–88.
Hudleston, P.J., 1973. An analysis of "single layer" folds developed experimentally in viscous media. Tectonophysics. 16, 189–214.
Ildefonse, B., Launeau, P., Bouchez, J.-L., Fernandez, A., 1992. Effect of mechanical interactions on the development of shape preferred orientations: a two-dimensional experimental approach. Journal of Structural Geology 14, 73–83.
Jeffery, G.B., 1922. The motion of ellipsoidal particles immersed in a viscous fluid. Proceedings of the Royal Society of London Series A 102, 161–179.
McKenzie, D.P., 1987. The compaction of igneous and sedimentary rocks. Journal of the Geological Society of London 144, 299–307.
Paterson, S.R., Vernon, R.H., Tobisch, O.T., 1989. A review of criteria for the identification of magmatic and tectonic foliations in granitoids. Journal of Structural Geology 11, 349–363.
Ramberg, H., 1963. Fluid dynamics of viscous buckling applicable to folding of layered rocks. American Association of Petroleum Geologists Bulletin 47, 484–505.
Ramsay, J.G., Huber, M.I., 1983. The Techniques of Modern Structural Geology, vol. 1. Academic Press, London.
Ramsay, J.G., Huber, M.I., 1987. The Techniques of Modern Structural Geology, vol. 2. Academic Press, London.
Ribeiro, A., Kullberg, M.C., Possolo, A., 1983. Finite strain estimation using 'anti-clustered' distributions of points. Journal of Structural Geology 5, 233–243.
Sen, S., 1956. Structures of the porphyritic granite and associated metamorphic rocks of east Manbhum, Binar, India. Geological Society of America Bulletin 67, 647–670.
Shelley, D., 1993. Igneous and Metamorphic Rocks Under the Microscope: Classification, Textures, Microstructures and Mineral Preferred Orientations. Chapman & Hall, London.
Smith, J.V., 1997. Shear thickening dilatancy in crystal-rich flows. Journal of Volcanology and Geothermal Research 79, 1–8.
Treagus, S.H., 1981. A theory of stress and strain variations in viscous layers and its geological implications. Tectonophysics 72, 75–103.
Vernon, R.H., 1991. Interpretation of microstructures of microgranitoid enclaves. In: Didier, J., Barbarin, B. (Eds.), Enclaves and Granite Petrology, Developments in Petrology 13. Elsevier, Amsterdam, pp. 277–291.
Vernon, R.H., Etheridge, M.A., Wall, V.J., 1988. Shape and microstructure of microgranitoid enclaves: indicators of magma mingling and flow. Lithos 22, 1–11.
Watters, W.A., 1962. Hornblende-rich gabbroic rocks from Cow and Calf Point, Stewart Island, New Zealand. Transactions of the Royal Society of New Zealand, Geology 1, 279–284.
Watters, W.A., 1978. Diorite and associated intrusive and metamorphic rocks between Port William and Paterson Inlet, Stewart Island, and on Ruapuke Island. New Zealand Journal of Geology and Geophysics 21, 423–442.
Wiebe, R.A., 1993. The Pleasant Bay layered gabbro-diorite, coastal Maine—ponding and crystallization of basaltic injections into a silicic magma chamber. Journal of Petrology 34, 461–489.
Wiebe, R.A., Collins, W.J., 1998. Depositional features and stratigraphic sections in granitic plutons: implications for the emplacement and crystallization of granitic magma. Journal of Structural Geology 20, 1273–1289.
Williams, Q., Tobisch, O.T., 1994. Microgranitic enclave shapes and magmatic strain histories: constraints from drop deformation theory. Journal of Geophysical Research 99, 24359–24368.